

# Histochemical and Morphometrical Analyses of Scarless Wound Healing in Mouse Fetal Model

Hiroshi KAWAKAMI<sup>\*1</sup>, Satoru NISHIZAWA<sup>\*2</sup>, Atsuhiko HIKITA<sup>\*3</sup> and Kazuto HOSHI<sup>\*1,3,4</sup>

<sup>\*1</sup>*Department of Sensory and Motor System Medicine, Graduate School of Medicine, The University of Tokyo*

<sup>\*2</sup>*Translational Research Center, The University of Tokyo Hospital*

<sup>\*3</sup>*Division of Tissue Engineering, The University of Tokyo Hospital*

<sup>\*4</sup>*Department of Oral-maxillofacial Surgery, Dentistry and Orthodontics, The University of Tokyo Hospital*

(Received January 6, 2021; Accepted January 7, 2021)

**Objective:** Scar formation is an inevitable outcome after craniofacial surgery in the congenital facial anomaly. Scarless healing is the ultimate treatment after the surgery. Therefore, we elucidate the mechanism underlying scarless healing during fetal development.

**Methods:** A full-thickness back skin excision (1 × 0.5 mm) was made at embryonic day 16.5 (E16.5) and 18.5 (E18.5) in fetal C57BL/6J mice and examined the histochemical and morphometrical findings of wound healing after 48 hours.

**Results:** The wound made at E16.5 showed almost complete re-epithelialization with fine reticular dermal collagen fibers, but not at E18.5. The ratio of CK5 positive area was significantly higher in the wound of E16.5 operation than in the E18.5. The wounds made at E18.5 showed granulation tissue formation which will lead to subsequent scar formation. The collagen fibers tended to be thinner in wound than in normal skin, while the decrease in the number of fibers but the increase in the straightness of fibers were evident in the wound at E18.5.

**Conclusion:** Transition point of scarless healing seemed between E16.5 and E18.5 in mice, which may imply that the potential of epithelial regeneration and matrix formation was changed, possibly due to alteration of cell constitution and decrease in stemness, at that time.

**Key words:** scarless healing, fetal surgery, epithelialization, scar transition point, macrophage

## INTRODUCTION

Scarless healing is the ultimate goal of surgical treatment. The outcomes of oral and maxillofacial surgery would be markedly improved by the development of scarless healing methods [1]. Wounds inflicted before a certain point during fetal development can heal without scar formation [2, 3]. In other words, the wound undergoes epithelialization without any scar tissue (e.g., collagen fibers with disturbed arrangement) in the dermis below the epithelium[4]. Additionally, regeneration of epidermal appendages, such as hair follicles and sebaceous glands, has been observed[5]. The capability of scarless healing is derived from intrinsic fetal tissue[6, 7] without external factors such as amniotic fluid [8, 9]. Based on extensive morphological analyses mainly in rat models, few inflammatory cytokines are involved [10], while less upregulation of wound-related transcriptional factors such as TGF- $\beta$ 1 and  $\beta$ 2 was noted [11]. Invasion by inflammatory cells such as macrophages are minimal [12], few myofibroblasts are involved in scarring contracture [13], and collagen fiber distribution is a uniform meshwork without any particular direction or bias [5]. Despite these insights, the exact mechanism of how scarless healing occurs remains unexplained.

Thus, it is critical to establish a model of scarless healing using mice. Mouse models are widely useful owing to their prevalence in disease research and their well-known genetic backgrounds. However, there have been no attempt in the literature to examine epithelialization and scar formation in detail in the mouse model, especially to reach detailed analysis of the size and arrangement of collagen fibers, which play a central role in scarring. The purpose of this study is to provide information on scarless wound healing, by histochemical analyses of epithelial cells or inflammatory cells and morphometrical evaluation of collagen fiber characteristics, in mouse fetal model.

To date, collagen fibers have been evaluated using an experimental system in which picrosirius red (PSR)-stained rat fetus models are imaged with fluorescent confocal microscopy. For this study, a spindle-shaped tissue defect (1 mm long × 0.5 mm wide) was created in the back skin of fetuses from pregnant mice (C57BL/6J) on either day E16.5 or E18.5. Fetuses were observed using Hematoxylin and Eosin (HE), Azan, and PSR staining (bright visual field, fluorescence), as well as immunostaining for CK5 and F4/80 to quantitatively analyze the changes occurring at about gestational age E18 (considered to be the transition point for scarless healing).

## MATERIALS AND METHODS

### Experimental animals

All experimental procedures were approved by the animal ethical committee of the University of Tokyo hospital (H20-039) and conducted according to the Guidelines for Animal Experiments at the Faculty of Medicine, the University of Tokyo, the Act on Welfare and Management of Animals, Standards Relating to the Care and Keeping and Reducing Pain of Laboratory Animals (Notice of the Ministry of the Environment), and the ARRIVE Guidelines.

Eight-week-old C57BL/6J strain mice were purchased from CLEA Japan (Tokyo, Japan) and mated at the Clinical Research Center animal facility at the University of Tokyo hospital. When a vaginal plug was observed, the noon of the same day was designated as embryonic day 0.5 (E0.5).

### Surgical procedure

Time dated E16.5 and E18.5 pregnant C57BL/6J mice were induced and maintained anesthesia by inhalation of 2% isoflurane (Pfizer Japan Inc., Tokyo, Japan). Mice were kept supine position, and the abdomen was sterilized by 70% ethanol and shaved. Laparotomy was performed with a midline abdominal incision. Both left and right uterus horns were pulled out of the abdominal cavity and the fetuses were identified and counted. Up to 5 fetuses per dam and up to 3 fetuses per unilateral uterus horn were operated to reduce the risk of preterm labor and fetal demise. Fetal dorsal skin was detected, taking advantage of amniotic fluid transparency. A 2–3 mm straight-line uterus incision was made just above the fetal dorsal skin to pull out of the fetus. A 7–0 pursue sling suture was performed around the uterus incision to minimize amniotic fluid loss during the procedure. Once the fetal dorsal skin was exposed, 1 mm length  $\times$  0.5 mm width full-thickness skin excision was applied by surgical scissors along the longitudinal axis. One hundred microliters of India ink was dropped onto the excisional site to ensure the same position after scarless healing (Fig. 1b, green arrowhead). Finally, the uterus incision and the abdominal incision were closed by a 7–0 pursued sling suture and an interrupted suture, respectively.

### Histology

Fetal mice were fixed by 4% paraformaldehyde in phosphate buffered saline (pH7.4) for about 3–7 days, depending on the fetus's embryonic day. Samples ( $n = 5$  (E16.5),  $n = 3$  (E18.5)) were horizontally cut in the middle of the torso and embedded in a paraffin block using standard methods. Paraffin sections were prepared in 5  $\mu$ m thickness using a Leica rotary microtome (Leica, RM2265) and stained with hematoxylin and eosin (HE) methods for general observation, Azan or picosirius red (PSR) methods for collagen observation. For the histological quantification, CK5 immunohistochemistry was performed to observe the regeneration of epidermal basal cell layer and F4/80 immunohistochemistry was done for inflammatory cells. Proteolytic-induced epitope retrieval (PIER) method for both CK5 and F4/80 were used. Briefly, for CK5, applied 200  $\mu$ l of 0.1% trypsin (gibco, 15090-046) in 1x PBS per each

sample and incubated for 20 minutes at 37 degrees Celsius. For F4/80, applied one drop of proteinase solution (NICHIREI CORPORATION, 415231) per each sample and incubated for 2 minutes at room temperature. The primary antibodies were CK5 (Abcam, ab53121, 1:5000) and F4/80 (Abcam, ab6640, 1:1000), and normal rabbit IgG (Abcam, ab172730, 1:5000) and normal rat IgG (FUJIFILM Wako Pure C., 147-09521, 1:1000) were used for the negative control, respectively. The secondary antibodies were goat anti-rabbit IgG for CK5 (NICHIREI CORPORATION, 426011) and anti-rat IgG for F4/80 (VECTOR, BA-4000), respectively. For the avidin-biotin complex (ABC) method, the VECTASTAIN<sup>®</sup> ELITE<sup>®</sup> ABC kit (VECTOR, PK-6100) was used. Avidin biotin complex was detected by the DAB Peroxidase Substrate Kit (VECTOR, SK-4100).

Glass slides were photographed by a BX51 epifluorescence microscope (OLYMPUS, Tokyo, Japan) with a DP74 digital CCD camera (OLYMPUS, Tokyo, Japan). TIFF data were saved by a CellSens (OLYMPUS, Tokyo, Japan) standard microscope software. All images were captured at 1600  $\times$  1200 resolution.

### Quantification

Immunohistochemistry and PSR images were quantified by ImageJ v1.42a [14]. For immunohistochemistry, TIFF data were converted to binarized images and extracted positive areas. For CK5, the ratio of the positive area was calculated, and for F4/80, positive cell numbers were counted. For PSR, fluorescence TIFF data was split into RGB channels, and the red channel, including PSR signals was binarized. Region of interest (ROI) was set correspondent to the excisional dermal area (800  $\times$  300 pixels; 13000  $\mu$ m<sup>2</sup>). Parameters for collagen fibers, including width, length, number, angle, and straightness, of the ROIs were analyzed by CT-FIRE v2.0 beta[15–17] fiber detection software with MatLab R2014b.

### Statistical analysis

All results were expressed as mean (SD). All statistical analyses were performed by R version 3.6.1 (R Foundation for Statistical Computing; Vienna, Austria). The equality of variance was confirmed by the *F*-test before Welch's test to compare two groups. The Tukey-Kramer test was performed as multiple comparisons. Sample sizes were not predetermined. The threshold for significance was set at  $P < 0.05$ .

## RESULTS

### Macroscopic features

Representative macroscopic findings upon harvest of the fetuses 48h after surgery are shown in Fig. 2. The epidermis of the E18.5 (E16.5 operated) fetuses had a smooth surface with no macroscopic distinction between the wound and the surrounding intact tissue. The wound could be identified by the penetration of India ink (used for marking at the time of operation) through the epidermis. In the E20.5 (E18.5 operated) fetuses, the wound was red and depressed, clearly differing from the surrounding intact epidermis. The India ink could not be clearly localized macroscopically.

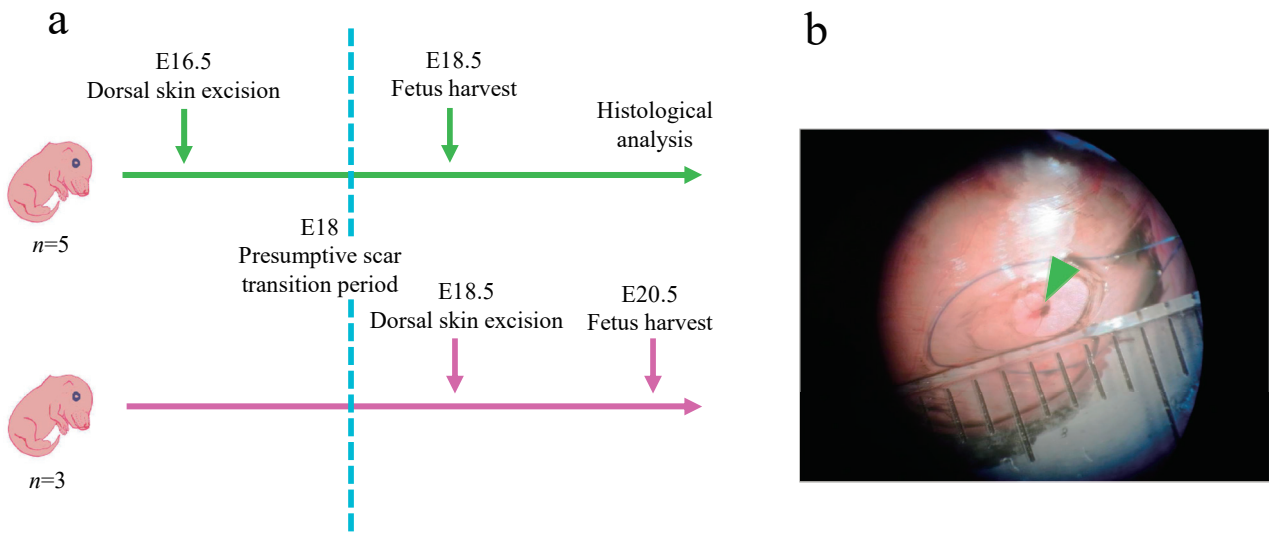
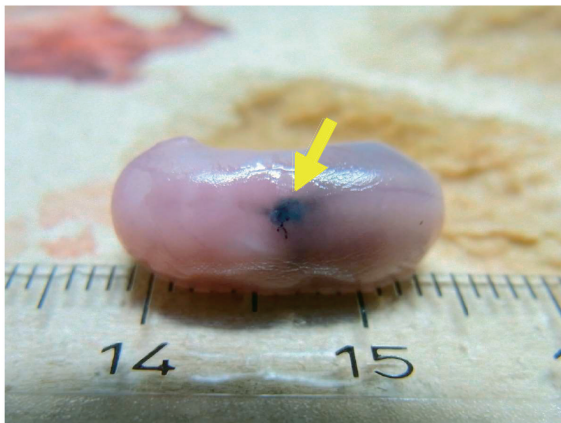


**Fig. 1** An overview of fetal dorsal excisional wound making.  
 a. Scheme of experimental design. We operated on fetuses before (E16.5,  $n = 5$ ) and after (E18.5,  $n = 3$ ) the presumptive scar transition period, harvested fetuses 48 hours after surgery, and analyzed them histologically.  
 b. Intraoperative photograph of the fetal dorsal skin under the dissection microscope (magnification 40x, 1 mm  $\times$  0.5 mm full-thickness excision). We drooped 100  $\mu$ l of India ink to confirm the wound site after scarless healing (green arrowhead).

E18.5 fetus  
(E16.5 operated)



E20.5 fetus  
(E18.5 operated)



**Fig. 2** Gross morphology  
 Left. The wound site at E16.5 operated fetuses was healed and indistinguishable compared to adjacent normal dorsal skin. The yellow arrow shows India ink through the healed epithelial tissue.  
 Right. The yellow arrow shows redness at the wound site at E18.5 operated fetuses.

### Histology

On the skin of wound which was marked by India ink in E18.5, the newly formed epidermis was observed (Fig. 3, E18.5 (E16.5 ope)). When stained with HE, keratinization was found in the newly formed epithelium at the wound (Fig. 3, E18.5 (E16.5 ope), HE), like in normal skin (Fig. 3, E18.5 normal skin, HE). Under higher magnification, basal cells seemed round or cuboidal, although cell polarity was not determined (Fig. 5, E18.5 (E16.5 ope)). Unlike the normal basal cell layer, nuclei of basal cells in the wound were irregularly arranged (Fig. 5, E18.5 (E16.5 ope)). Some sections showed an accumulation of histiocyte-like cells around the India ink, and also disclosed the areas with a high density of small vessels and vascular endothelial cells. Limited granulation was observed throughout the

visual field. Azan staining (Fig. 3, Azan) revealed that collagen fibers were stained with aniline blue, and that ones were visible around the India ink immediately below the newly formed epithelium (Fig. 3, E18.5 (E16.5 ope), Azan). When examined by PSR staining, arrangement of collagen fibers was stained in red or magenta under either bright field and fluorescent observation, respectively (Fig. 3, PRS). Collagen fibers both in the normal skin (Fig. 3, E18.5 normal skin, PRS) and in the wound (Fig. 3, E18.5 (E16.5 ope), PRS) tended to be thin and waved.

In the E20.5 (E18.5 operated) skin, epithelialization was incomplete (Fig. 4, E20.5 (E18.5 ope)). While normal basal cell layer was not observed in the wound (yellow arrowhead in Fig. 4, E20.5 (E18.5 ope), HE), the wound was mostly covered with a fibrin-like struc-

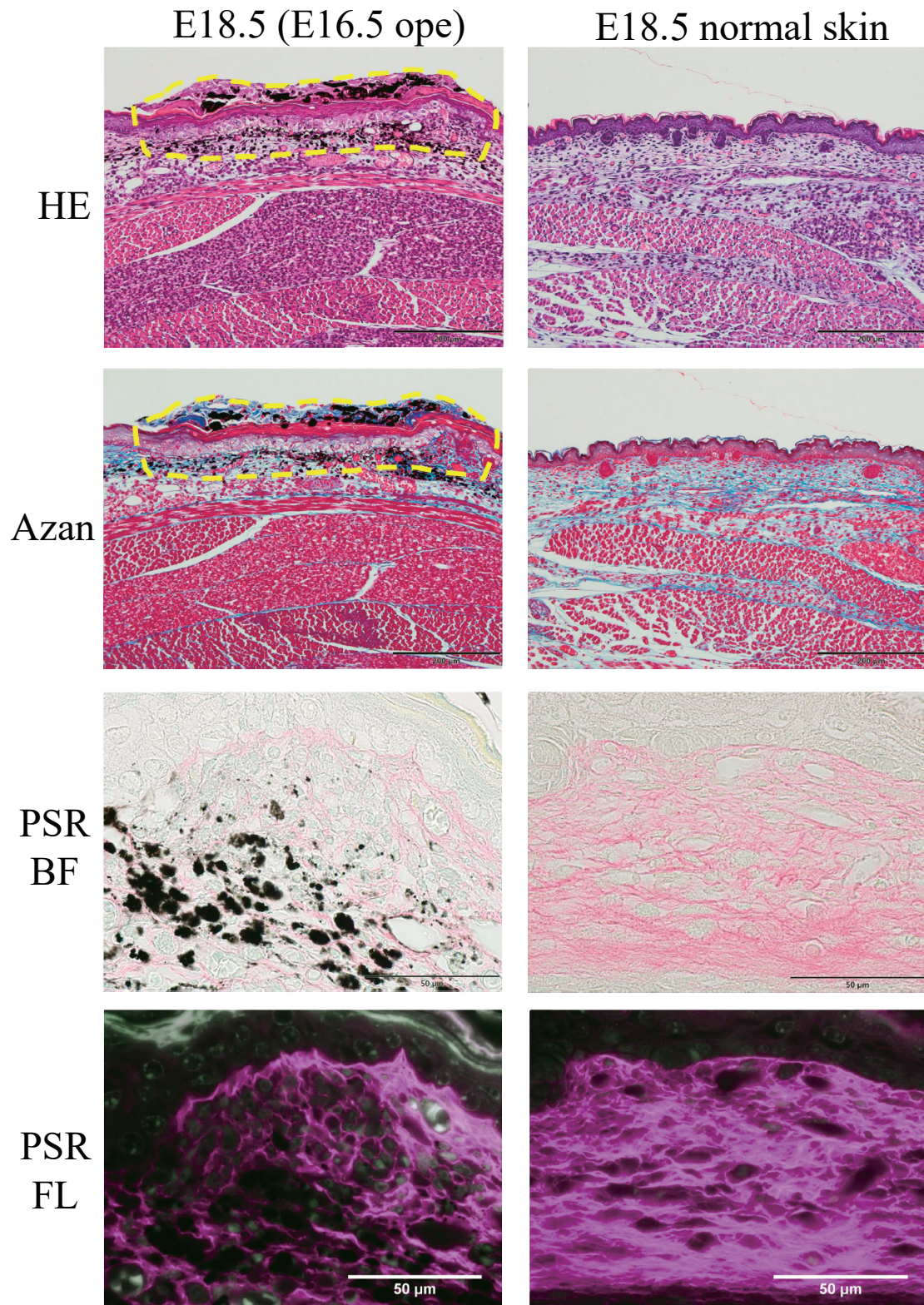


**Fig. 3** Histological findings of E18.5 (E16.5 operated) fetus. The Left column represents E18.5 wound tissue, and the right column represents E18.5 normal skin tissue. Each row showed HE, Azan, PSR bright field, and PSR fluorescence image. The wound was covered by the newly formed epithelium. Collagen fibers under the newly formed epithelium showed a fine reticular pattern and indistinguishable from adjacent normal dermal tissue. Scalebar: 200  $\mu\text{m}$  (20x), 50  $\mu\text{m}$  (100x).

ture (yellow arrowhead in Fig. 4, E20.5 (E18.5 ope), Azan). Granulation could be observed at the wound edge (Fig. 5, E20.5 (E18.5)). These granulation tissues comprised small-diameter cells that seemingly included histiocytes, vascular endothelial cells, and fibroblasts.

Azan staining revealed positive staining of the fibrin-like structure with azocarmine G (yellow arrowhead in Fig. 4, E20.5 (E18.5 ope), Azan). Immediately below this structure, collagen fibers were shown at and around the bottom of the wound (Fig. 4, E20.5 (E18.5

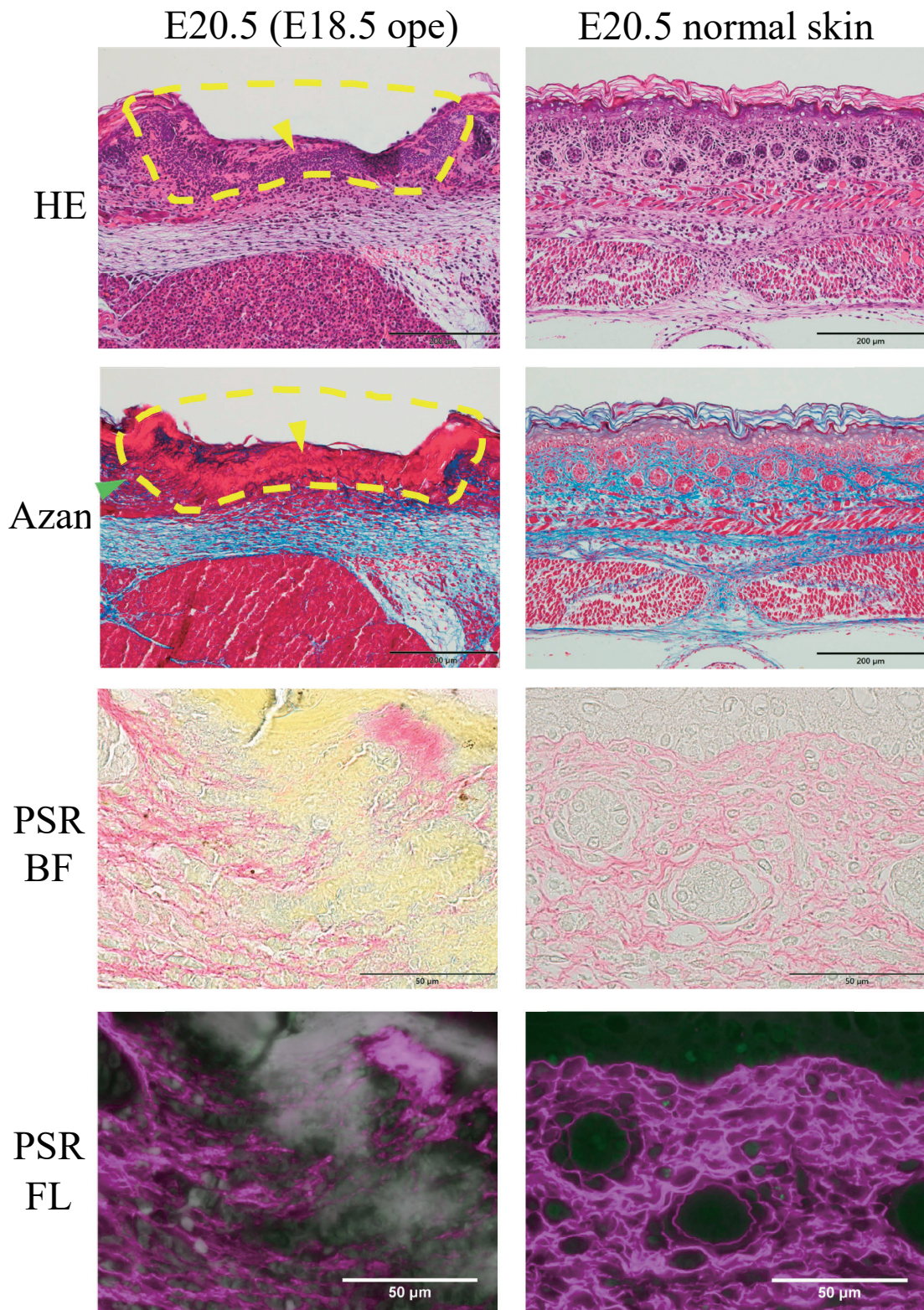


**Fig. 4** Fig. Histological findings of E20.5 (E18.5 operated) fetus. The Left column represents E20.5 wound tissue, and the right column represents E20.5 normal skin tissue. Each row showed HE, Azan, PSR bright field, and PSR fluorescence image. The fibrin-like structure covered the wound. Scalebar: 200  $\mu\text{m}$  (20x), 50  $\mu\text{m}$  (100x).

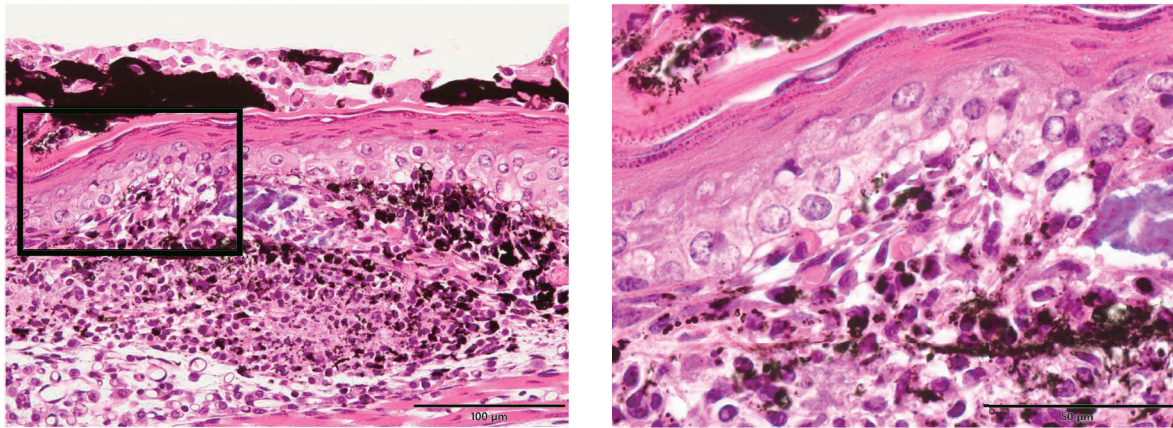
ope), PSR), although those were arranged below the dermis in the normal skin (Fig. 4, E20.5 normal skin, PSR). Both Azan and PSR staining revealed that collagen fibers showed rather straight arrangement within the subdermal layer at the wound edge (Fig. 4, E20.5 (E18.5 ope) Azan green arrow and PSR).

### Immunohistochemistry

#### CK5

In the E18.5 (E16.5 operated) skin, CK5 was distributed contiguously, consistent with its presence in the basal cell layer (Fig. 6). The localization of CK5 was a little thicker in wound (Fig. 6, E18.5 (E16.5 ope)) than that in normal skin (Fig. 6, E18.5 normal). In the

## E18.5 (E16.5 ope)



## E20.5 (E18.5 ope)

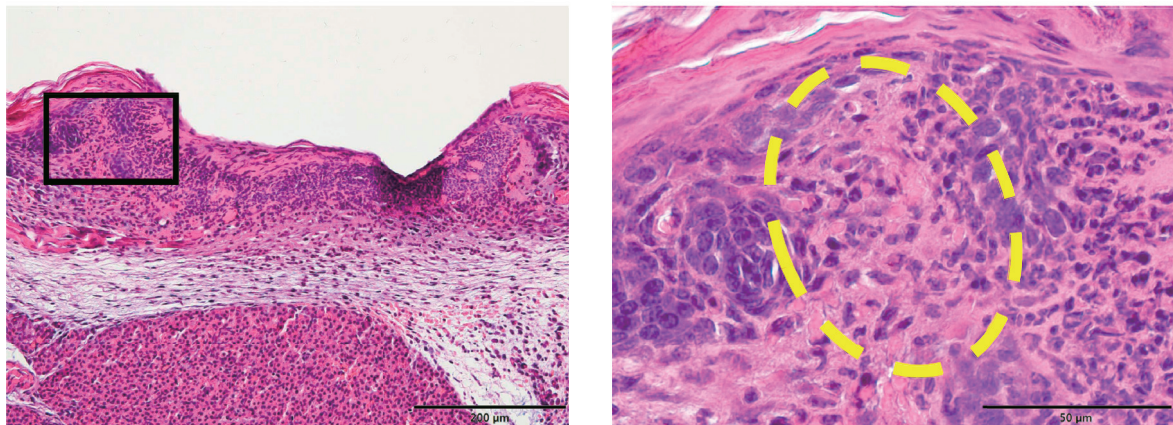


**Fig. 5** High-power field of HE stained wound healing area (observation of same samples as Fig. 3 and 4). Basal cells showed enlarged cytoplasm and nucleus with vacuolization in E18.5 fetuses. Phagocytosis of India ink can be observed by histiocyte-like cells in the dermal layer and keratinocyte in the horny layer over the healed epithelium (right is high magnification of left). In contrast, no basal cell was observed, and dense fibrin like tissue covered the wound in E20.5 fetuses. Small-diameter histiocytes like cells, vascular endothelial cells, and fibroblast-like cells accumulation were observed in wound edge (dotted circle) (right is high magnification of left). These findings indicate granulation tissue formation, which will lead to subsequent scar formation. Scalebar: upper left 200  $\mu\text{m}$  (20x), lower left 100  $\mu\text{m}$  (40x), upper and lower right 50  $\mu\text{m}$  (100x).

wound of E20.5 (E18.5 operated), few CK5 positive basal cells were noted (Fig. 6, E20.5).

### F4/80

In the E18.5 (E16.5 operated) skin, F4/80 positive cells were distributed sporadically around the India ink (Fig. 7, E18.5 (E16.5 ope)). In the normal skin of E18.5 fetuses, F4/80 positive cells were also observed in the dermis (Fig. 7, E18.5 normal skin). In E20.5 (E18.5 operated) skin, F4/80 positive cells were distributed sporadically at the wound edge (Fig. 7, E20.5 (E18.5 ope)). Although F4/80 signals were weak in fetal skin samples, we confirmed strong positive signals in the adult C57BL/6J liver tissue (Supplementary Fig. 1).

### IHC and collagen fiber quantification

The ratio of CK5 positive area was significantly higher in the E18.5 fetuses (2.24 (0.95) a.u.) than in the E20.5 fetuses (0.48 (0.11) a.u.) ( $P = 0.036$ , Fig. 8a). Although the number of F4/80 positive cells was significantly higher in the operated skin (388 (139) cells) than that of normal skin (146 (77) cells) in E18.5 ( $P = 0.014$ ), that difference was not found in E20.5 (Fig. 8a).

The collagen fiber width of the E18.5 (E16.5 operated) skin was smaller in the wound (1.43 (0.05)  $\mu\text{m}$ ) than in the normal skin area (1.57 (0.05)  $\mu\text{m}$ ) ( $P = 0.0075$ ). This was also the case in the E20.5 (E18.5 operated) skin; collagen fiber was smaller in

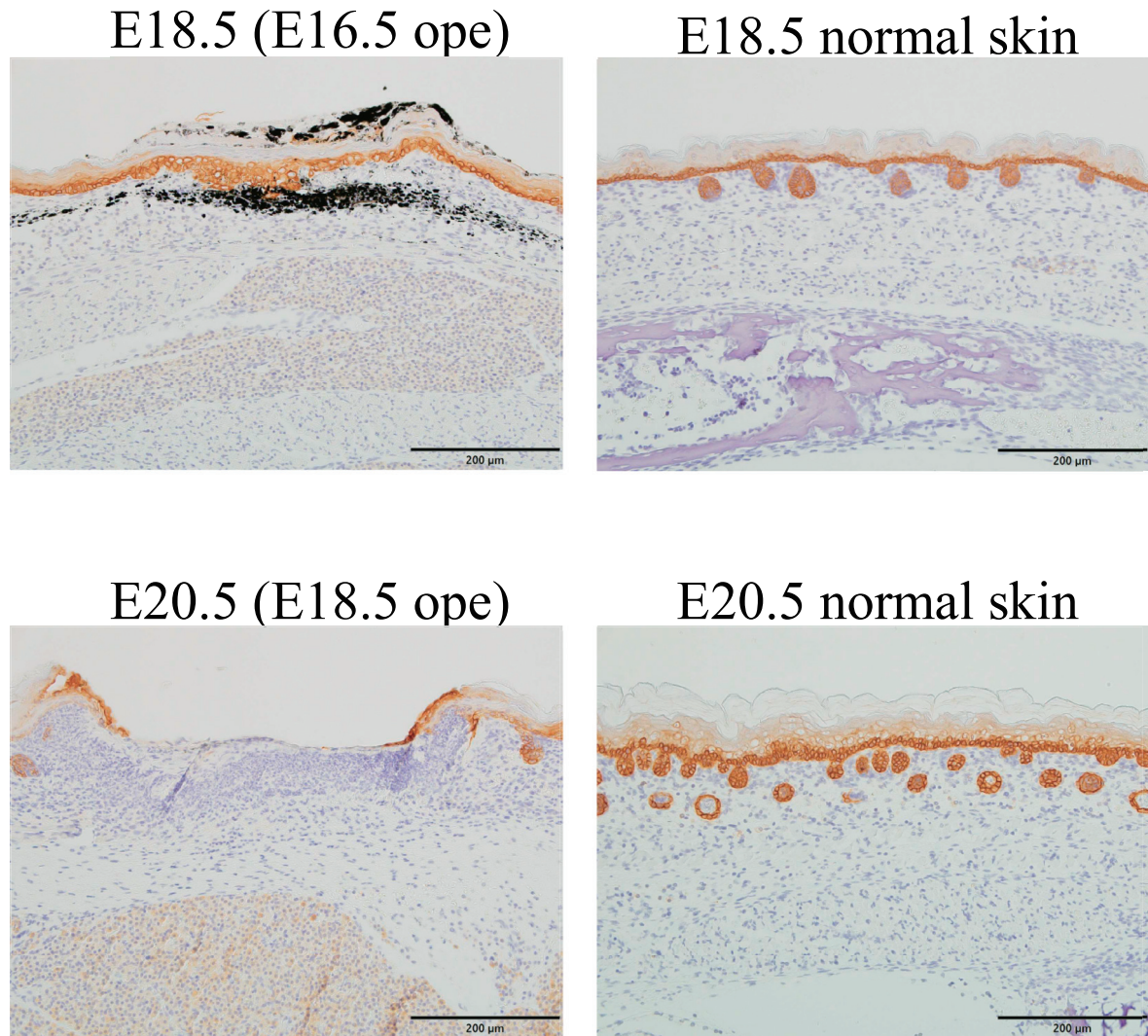


**Fig. 6** Immunohistochemical localization of cytokeratin5 (CK5). CK5 immunohistochemical staining of the fetal dorsal skin excisional wound 48 hours after surgery. The upper row showed E18.5 fetuses, and the lower showed E20.5. Almost complete epithelialization with several layers of basal cell were found in E18.5 fetuses, whereas no basal cell migration was observed in E20.5 fetuses. Representative photographs were shown in the figure ( $n = 5$  (E18.5),  $n = 3$  (E20.5)). Scalebar: 200  $\mu\text{m}$  (20x).

the wound (1.40 (0.08)  $\mu\text{m}$ ) than in the intact area (1.57 (0.05)  $\mu\text{m}$ ) ( $P = 0.017$ ). The collagen fiber length of the E20.5 (E18.5 operated) skin (7.91 (0.75)  $\mu\text{m}$ ) was smaller than that of E18.5 normal skin (8.65 (0.53)  $\mu\text{m}$ ) ( $P = 0.047$ ). The number of collagen fibers was significantly less in the wounds of E20.5 (E18.5 operated) skin (240 (63)/ROI) than in the wounds of E18.5 (E16.5 operated) skin (589 (130)/ROI) and in the normal skin areas of E18.5 (553 (116)/ROI) and E20.5 (653 (43)/ROI) ( $P = 0.0012, 0.0027, 0.0009$ ) (Fig. 8b). There was no intergroup difference in angle. The differences in the straightness of collagen fibers were negligible small but statistically higher in the E20.5 (E18.5 operated) skin than E18.5 normal skin, E18.5(E16.5 operated) skin, and E20.5 normal skin, respectively ( $P = 0.026, 0.026, 0.047$ ) (Fig. 8b).

#### DISCUSSION

The morphological differences of the basal cell layer in the newly formed epithelium from that in the other areas seem to reflect regeneration. In an experiment using BALB/c mice [18], epithelialization seems to

have occurred at least 48 h after wounding in both E18.5 (E16.5 operated) and E20.5 (E18.5 operated) skin. In another experiment using rats [5], 100% healing was achieved 72 h after the operation in E16.5 fetuses, while only 50% healing was achieved in E18.5 fetuses after the same amount of time. In the present study, epithelialization occurred in all E18.5 (E16.5 operated) skin, while epithelialization was incomplete in all E20.5 (E18.5 operated) skin. In E18.5 (E16.5 operated) skin, the basal cells of the wound had larger nuclei and expanded cytoplasm were oval-shaped, and showed disturbing polarity compared to basal cells in the intact area. In the E20.5 (E18.5 operated) skin, migration of basal cells from the wound edge was observed, but the wound was not completely covered.

This suggests that either migration of epidermal cells occurs considerably earlier in E18.5 (E16.5 operated) skin than in E20.5 (E18.5 operated) skin or that regeneration of the epithelium occurs by a mechanism different from migration from the basal cell layer at the wound edge. When the tissue around the wound was observed at low magnification, a group of juvenile

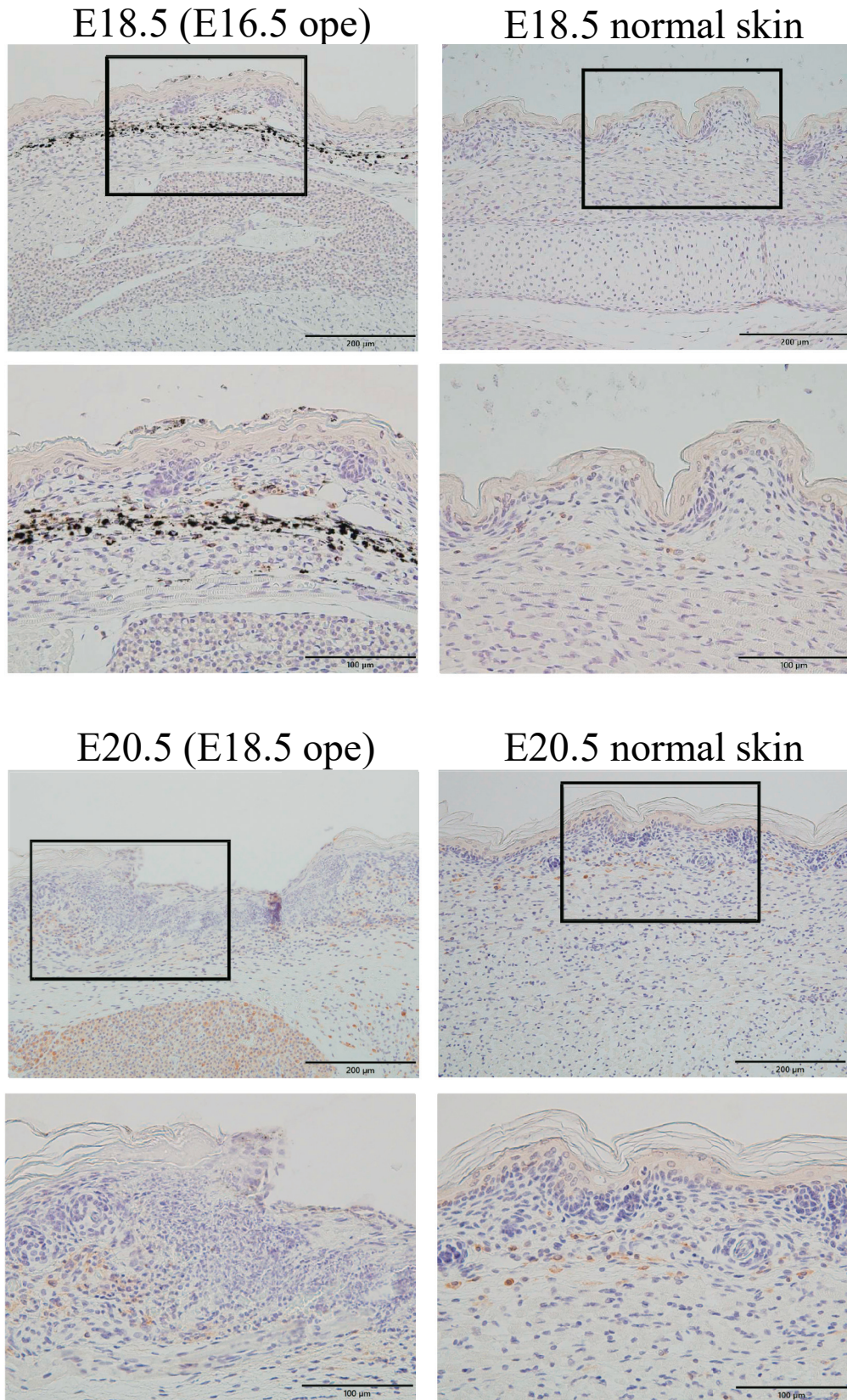


**Fig. 7** Immunohistochemical localization of F4/80 positive cells. F4/80 immunohistochemical staining of the fetal dorsal skin excisional wound 48hours after surgery. a: The upper row showed E18.5 fetuses, and the lower showed E20.5. The number of F4/80 positive cells significantly higher in the E18.5 (E16.5 operated) skin than in the E18.5 normal skin. Representative photographs were shown in the figure ( $n = 5$  (E18.5),  $n = 3$  (E20.5)). Scalebar: upper row; 200 µm (20x), lower row; 100 µm (40x).

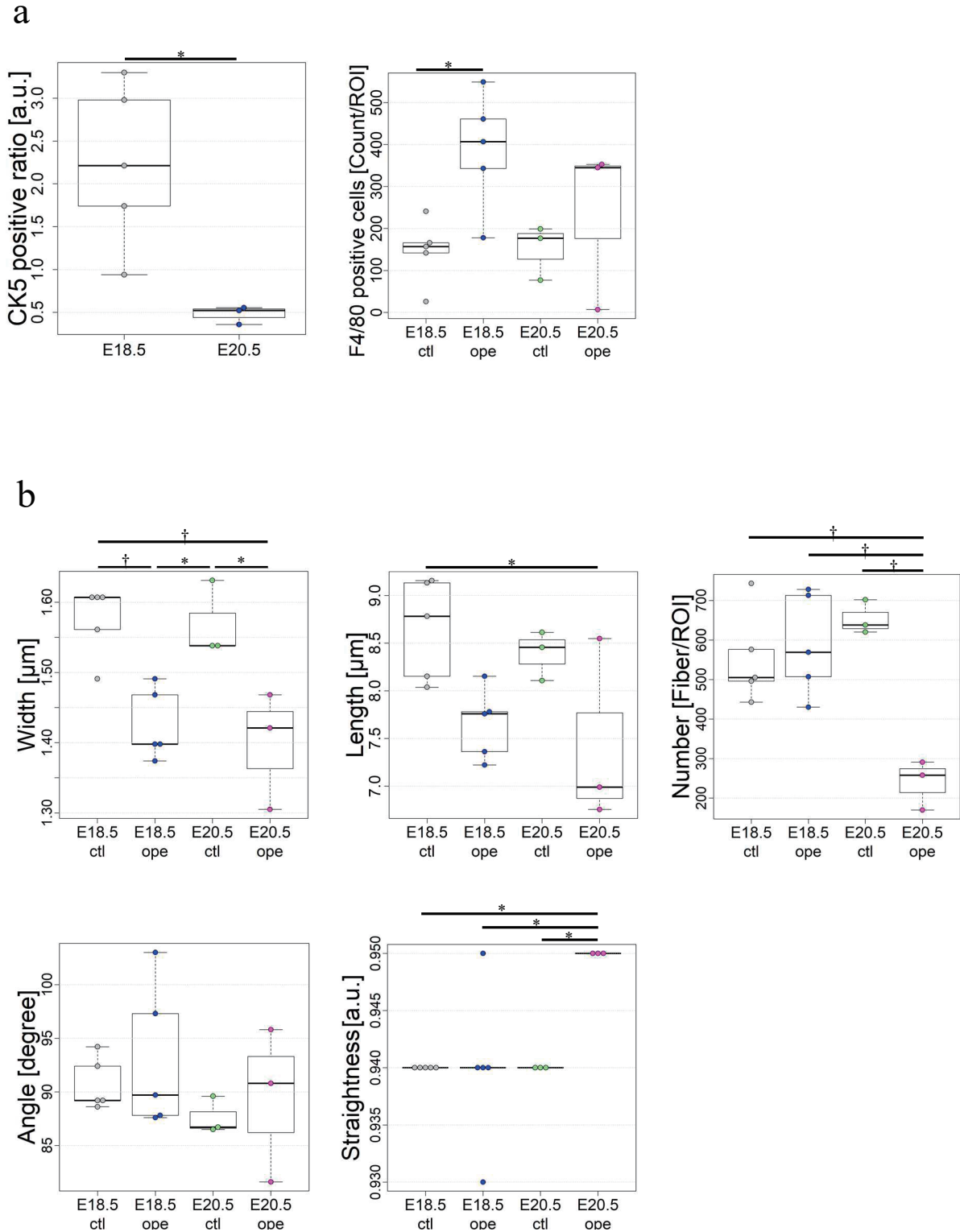
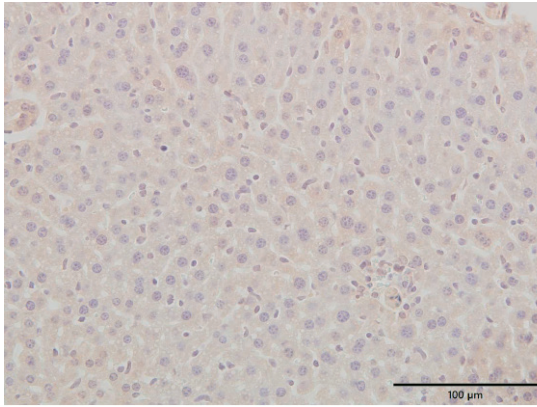


**Fig. 8** Histochemical and morphometrical analysis

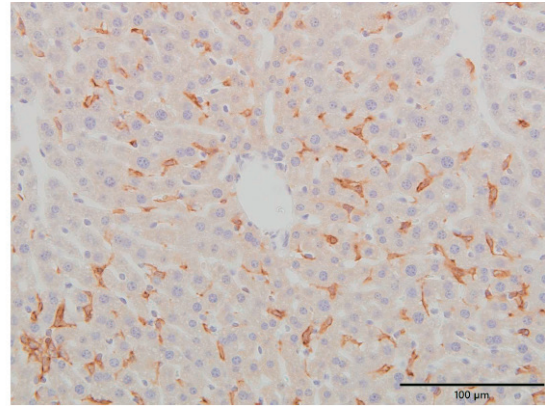
a. quantification of immunohistochemistry. The CK5 positive area ratio was significantly higher in the E18.5 fetuses (2.24 (0.95)) than in the E20.5 fetuses (0.48 (0.11)) ( $P = 0.036$ ). The number of F4/80 positive cells was significantly higher in the E18.5 (E16.5 operated) skin (388 (139) cells) than that of E18.5 normal skin (146 (77) cells) ( $P = 0.014$ ).

b. quantitative analysis of the parameters of collagen fibers. The collagen fiber width of the E18.5 (E16.5 operated) skin was smaller in the wound (1.43 (0.05)  $\mu\text{m}$ ) than in the normal skin area (1.57 (0.05)  $\mu\text{m}$ ) ( $P = 0.0075$ ). This was also the case in the E20.5 (E18.5 operated) skin; collagen fiber was smaller in the wound (1.40 (0.08)  $\mu\text{m}$ ) than in the normal skin area (1.57 (0.05)  $\mu\text{m}$ ) ( $P = 0.017$ ). The collagen fiber length of the E20.5 (E18.5 operated) skin (7.91 (0.75)  $\mu\text{m}$ ) was smaller than that of E18.5 normal skin (8.65 (0.53)  $\mu\text{m}$ ) ( $P = 0.047$ ). The number of collagen fibers was significantly less in the wounds of E20.5 (E18.5 operated) skin (240(63)/ROI) than in the wounds of E18.5 (E16.5 operated) skin (589 (130)/ROI) and in the normal skins of E18.5 (553 (116)/ROI) and E20.5 (653 (43)/ROI) ( $P = 0.0012, 0.0027, 0.0009$ ). The Tukey-Kramer test was performed for multiple comparisons ( $n = 5$  (E18.5),  $n = 3$  (E20.5)). \*:  $P < 0.05$ , †:  $P < 0.01$

## Normal IgG



## F4/80



**Supplementary Fig. 1** adult C57BL/6J liver histology  
F4/80 positive cells (Kupffer cells) in the liver tissue can be observed in positive control samples. In contrast, F4/80 signals were not observed in negative control samples. Scalebar: 100  $\mu$ m(40x).

cells (not resembling the cells constituting muscle or fat tissue) was found below the dermis of E18.5 (E16.5 operated) skin but not in the E20.5 (E18.5 operated) skin. These cells are considered to represent premature mesenchymal cells under development. Therefore, it is possible that in E18.5 (E16.5 operated) skin, premature mesenchymal cells or those with high stemness are directly recruited to the wound, resulting in the formation of new epithelium.

In E18.5 (E16.5 operated) skin, cells that incorporated the India ink were found in both the horny layer of newly formed epithelium and the tissue below the newly formed basal cell layer, while India ink incorporation was not observed from the newly formed basal cell layer to the granulocyte layer. If the mesenchymal cells of the subdermal tissue differentiated into the epithelium, India ink should have been incorporated in all of the subdermal, basal cell, and horny layers. However, this was not observed in any of these layers. In E20.5 (E18.5 operated) skin, however, epithelialization through cell migration hardly occurred, and it seems unlikely that a wound of about 0.5 mm width can be completely covered by cell migration only 48 h after wounding. Furthermore, in the E18.5 (E16.5 operated) skin, if epithelialization occurs through cell migration, gradation of differentiation from the center to the edge of the wound should have been observed. However, the newly formed epithelium did not resemble the basal cells, that is, a uniform bubble-like shape from one end of the wound to the other.

To determine the origin of newly formed basal cells, it is necessary to conduct observations at time points during a short period after wound creation. Furthermore, as complete epithelialization is unlikely to occur within 48 h after wound creation, a longer follow-up is needed to determine the final outcome of scarring. Therefore, conducting both short-term and long-term observations will contribute to the elucidation of the exact mechanism of new epithelium formation.

The extent of epithelialization in the present study partially differed from that shown in previous reports. One possible cause for this is the difference in healing

reactions to wounds among different mouse strains. In this regard, a study on wound healing in three strains of mice (C57BL/6J, BALB/c, and MRL) reported that skin wounding resulted in scar formation in each strain, while regeneration ear wounds only occurred in MRL mice [19]. However, that study used mature mice, and different results may be obtained in fetuses.

Collagen fiber formation is also involved in scarring. In E18.5 (E16.5 operated) skin, the width of collagen fibers differed significantly between the wound and the intact area, but no significant difference was noted in any other parameters such as length, angle, number, or linearity. Consistent with the macroscopic observations, this indicates that the generation of collagen fibers in the wound area is similar to that seen in the intact area. In E20.5 (E18.5 operated) skin, the width and number of collagen fibers differed significantly between the wound and the intact area, although there was no significant difference in the other parameters such as length, angle, or linearity (the absolute number of collagen fibers was low in these fetuses). This outcome can be explained by the following: (1) the wound was filled with a fibrin-like structure mentioned above and had not undergone epithelialization, and (2) few new collagen fibers had formed.

It has been reported that scarless healing involves less infiltration of inflammatory cells. According to a previous report, macrophages are recruited to the site of tissue repair after gestational age E14.5 [20]. In this study, the number of F4/80 positive cells significantly higher in the E18.5 (E16.5 operated) skin than in the E18.5 normal skin. When examined by HE staining, accumulation of cells seemingly representing histiocytes was noted in E20.5 (E18.5 operated). This appears to represent a group of F4/80 negative cells. In recent years, close attention has been paid to macrophage subtype analysis, and reports have been published on various markers of M1 and M2 macrophages. To date, however, there seems to be no report on the analysis of macrophage subtypes in relation to scarless healing. This type of study is clearly needed.

Although there exist several reports concerning scarless healing of the back skin in fetuses, reports on

scarless healing of fetal lips are scant and are confined to morphological observation [21–24]. Studies on lip healing need to be carried out using strains similar to those employed in studies of back skin healing. Previous studies have involved observation with HE staining over time and morphological observation through immunostaining of various types of extracellular matrix (ECM), but there seem to be no published studies focusing on lip muscle regeneration. Our ultimate goal is to establish a method for treating fetuses with cleft lip, including developing a method of muscle regeneration. To this end, observation and quantitative evaluation of lip muscle regeneration are necessary. We have already taken initial steps toward this goal and plan to publish reports in the near future.

As stated above, we intend to create a mouse model of surgically created cleft lip and to use this model for studies on scarless healing and fetal treatment. We will establish an experimental system in which a tissue defect is surgically created in the lips of mouse fetuses before the transition point and, after a period of spontaneous healing, the therapeutic intervention will be made to the healed wound (viewed as cleft lip). Such a model of the surgically created cleft lip has been reported for large animals (e.g., sheep), which have a long period of pregnancy but have not been reported for small animals such as mice. This is because a two-step therapeutic intervention (model creation and subsequent treatment) is difficult in mice with a short gestation period. The results from the present study indicate that most tissue defects of approximately 1 mm in size can heal within 48 h. Therefore, it appears possible to create and utilize a model of surgically created cleft lip in mice. We intend to report the establishment of such a model in the near future.

#### ACKNOWLEDGMENTS

We express our gratitude to Dr. Yutaka Takazawa, department of pathology, Toranomon Hospital, for giving us valuable histological implications. This work was supported by JSPS KAKENHI Grant Number JP17K19745 (Grant-in-Aid for Exploratory Research).

#### CONFLICT OF INTEREST

The authors declare that they have no conflicts of interest.

#### REFERENCE

- 1) A. Gimenez, R. Kopkin, D. K. Chang, M. Belfort, and E. M. Reece, "Advances in Fetal Surgery: Current and Future Relevance in Plastic Surgery," *Semin. Plast. Surg.*, vol. 33, no. 3, pp. 204–212, 2019.
- 2) J. D. Burrington, "Wound healing in the fetal lamb," *J. Pediatr. Surg.*, vol. 6, no. 5, pp. 523–528, 1971.
- 3) U. Rowlatt, "Intrauterine wound healing in a 20 week human fetus," *Virchows Arch. A Pathol. Anat. Histol.*, vol. 381, no. 3, pp. 353–361, 1979.
- 4) A. L. Moore, C. D. Marshall, L. A. Barnes, M. P. Murphy, R. C. Ransom, and M. T. Longaker, "Scarless wound healing: Transitioning from fetal research to regenerative healing," *Wiley Interdiscip. Rev. Dev. Biol.*, vol. 7, no. 2, Mar. 2018.
- 5) S. R. Beanes *et al.*, "Confocal microscopic analysis of scarless repair in the fetal rat: Defining the transition," *Plast. Reconstr. Surg.*, vol. 109, no. 1, pp. 160–170, 2002.

- 6) M. T. Longaker, D. J. Whitby, M. W. J. Ferguson, H. P. Lorenz, M. R. Harrison, and N. S. Adzick, "Adult skin wounds in the fetal environment heal with scar formation," *Ann. Surg.*, vol. 219, no. 1, pp. 65–72, 1994.
- 7) H. P. Lorenz, M. T. Longaker, L. A. Perkocho, R. W. Jennings, M. R. Harrison, and N. S. Adzick, "Scarless wound repair: A human fetal skin model," *Development*, vol. 114, no. 1, pp. 253–259, 1992.
- 8) J. R. Armstrong and M. W. J. Ferguson, "Ontogeny of the skin and the transition from scar-free to scarring phenotype during wound healing in the pouch young of a marsupial, *Monodelphis domestica*," *Developmental Biology*, vol. 169, no. 1, pp. 242–260, 1995.
- 9) M. A. Sancho, V. Juliá, A. Albert, F. Díaz, and L. Morales, "Effect of the environment on fetal skin wound healing," *J. Pediatr. Surg.*, vol. 32, no. 5, pp. 663–666, 1997.
- 10) A. King, S. Balaji, L. D. Le, T. M. Crombleholme, and S. G. Keswani, "Regenerative Wound Healing: The Role of Interleukin-10," *Adv. Wound Care*, vol. 3, no. 4, pp. 315–323, 2014.
- 11) D. J. Whitby and M. W. J. Ferguson, "Immunohistochemical localization of growth factors in fetal wound healing," *Dev. Biol.*, vol. 147, no. 1, pp. 207–215, 1991.
- 12) A. J. Cowin, M. P. Brosnan, T. M. Holmes, and M. W. J. Ferguson, "Endogenous inflammatory response to dermal wound healing in the fetal and adult mouse," *Dev. Dyn.*, vol. 212, no. 3, pp. 385–393, 1998.
- 13) J. M. Estes, J. S. V. Berg, N. S. Adzick, T. E. MacGillivray, A. Desmoulière, and G. Gabbiani, "Phenotypic and functional features of myofibroblasts in sheep fetal wounds," *Differentiation*, vol. 56, no. 3, pp. 173–181, 1994.
- 14) C. A. Schneider, W. S. Rasband, and K. W. Eliceiri, "NIH Image to ImageJ: 25 years of image analysis," *Nat. Methods*, vol. 9, no. 7, pp. 671–675, 2012.
- 15) C. R. Drifka *et al.*, "Comparison of Picrosirius Red Staining With Second Harmonic Generation Imaging for the Quantification of Clinically Relevant Collagen Fiber Features in Histopathology Samples," *J. Histochem. Cytochem.*, vol. 64, no. 9, pp. 519–529, 2016.
- 16) K. A. Wegner, A. Keikhosravi, K. W. Eliceiri, and C. M. Vezina, "Fluorescence of Picrosirius Red Multiplexed With Immunohistochemistry for the Quantitative Assessment of Collagen in Tissue Sections," *J. Histochem. Cytochem.*, vol. 65, no. 8, pp. 479–490, 2017.
- 17) J. S. Bredfeldt *et al.*, "Computational segmentation of collagen fibers from second-harmonic generation images of breast cancer," *J. Biomed. Opt.*, vol. 19, no. 1, p. 016007, 2014.
- 18) A. S. Colwell, T. M. Krummel, M. T. Longaker, and H. P. Lorenz, "An in vivo mouse excisional wound model of scarless healing," *Plast. Reconstr. Surg.*, vol. 117, no. 7, pp. 2292–2296, 2006.
- 19) A. S. Colwell, T. M. Krummel, W. Kong, M. T. Longaker, and H. P. Lorenz, "Skin wounds in the MRL/MPJ mouse heal with scar," *Wound repair Regen. Off. Publ. Wound Heal. Soc. [and] Eur. Tissue Repair Soc.*, vol. 14, no. 1, pp. 81–90, 2006.
- 20) J. Hopkinson-Woolley, D. Hughes, S. Gordon, and P. Martin, "Macrophage recruitment during limb development and wound healing in the embryonic and foetal mouse," *J. Cell Sci.*, vol. 107, no. 5, pp. 1159–1167, 1994.
- 21) A. R. Rowsell, "The intra-uterine healing of foetal muscle wounds: experimental study in the rat," *Br. J. Plast. Surg.*, vol. 37, no. 4, pp. 635–642, 1984.
- 22) D. J. Whitby and M. W. J. Ferguson, "The extracellular matrix of lip wounds in fetal, neonatal and adult mice," *Development*, vol. 112, no. 2, pp. 651–668, 1991.
- 23) K. Kohama, K. Nonaka, T. Nagata, K. Ogata, R. Hosokawa, and M. Ohishi, "[A study of the feasibility and efficacy of fetal surgical closure of spontaneous cleft lip in CL/fraser mice]," *Fukuoka Igaku Zasshi*, vol. 93, no. 1, pp. 11–16, Jan. 2002.
- 24) B. W. Robinson and A. N. Goss, "Intra-uterine healing of fetal rat cheek wounds," *Cleft Palate J.*, vol. 18, no. 4, pp. 251–255, Oct. 1981.